The Astrophysical Journal, 794:60 (11pp), 2014 October 10 doi:10.1088/0004-637X/794/1/60

RED GIANT STARS FROM THE SLOAN DIGITAL SKY SURVEY. II. DISTANCES

Kefeng Tan, Yuqin Chen, Kenneth Carrell, Jingkun Zhao, and Gang Zhao
Key Laboratory of Optical Astronomy, National Astronomical Observatories, Chinese Academy of Sciences, Beijing 100012, China; tan@nao.cas.cn
Received 2014 March 27; accepted 2014 August 12; published 2014 September 24

ABSTRACT

We present distance determinations for a large and clean sample of red giant branch stars selected from the ninth data release of the Sloan Digital Sky Survey. The distances are calculated based on both observational cluster fiducials and theoretical isochrones. Distributions of distances from the two methods are very similar with peaks at about 10 kpc and tails extending to more than 70 kpc. We find that distances from the two methods agree well for the majority of the sample stars; though, on average, distances based on isochrones are 10% higher than those based on fiducials. We test the accuracy of our distance determinations using 332 stars from 10 Galactic globular and open clusters. The average relative deviation from the literature cluster distances is 4% for the fiducial-based distances and 8% for the isochrone-based distances, both of which are within the uncertainties. We find that the effective temperature and surface gravity derived from low-resolution spectra are not accurate enough to essentially improve the performance of distance determinations. However, for stars with significant extinction, effective temperature may help to better constrain their distances to some extent. We make our sample stars and their distances available from an online catalog. The catalog comprises 17,941 stars with reasonable distance estimations reaching to more than 70 kpc, which is suitable for the investigation of the formation and evolution of the Galaxy, especially the Galactic halo.

Key words: Galaxy: stellar content – stars: distances

Online-only material: color figures, machine-readable table

1. INTRODUCTION

During the last decade, stellar content of large surveys, such as the Sloan Digital Sky Survey (SDSS; York et al. 2000) and the Radial Velocity Experiment (RAVE; Steinmetz et al. 2006), has been extensively used to study the formation and evolution of the Milky Way (e.g., Ivezić et al. 2008; Carollo et al. 2010; Lee et al. 2011b; Wilson et al. 2011; Kordopatis et al. 2013b; Binney et al. 2014b). The ongoing LAMOST (Large sky Area Multi-Object fiber Spectroscopic Telescope, also known as the Guoshoujing telescope, see Cui et al. 2012 for details) survey will provide spectra for more than 10 million Galactic stars, which will allow us to investigate the Galaxy in unprecedented detail (Zhao et al. 2012). The distances to individual stars plays a very important role in building the three-dimensional structure of the Galaxy, based on which the kinematics and metallicity distributions of the stars can be obtained and further used to trace the formation and evolution history of the Galaxy.

The most direct method for distance determination, i.e., the trigonometric parallax technique, could only be applied to very bright stars within several hundred parsecs to the Sun for the time being (Perryman et al. 1997). To probe more distant stars, we must rely on the photometric distances (Beers et al. 2000; Jurić et al. 2008), which are derived by inferring the absolute magnitudes from colors and observational or theoretical color–magnitude diagrams (CMDs). Both of the observational and theoretical CMDs have advantages and disadvantages in the determination of distances. Observational CMDs usually come from stellar cluster fiducial sequences (e.g., Brown et al. 2005; Clem et al. 2008; An et al. 2008). Each sequence represents a population of stars with the same age and metallicity, but different masses. However, only several fiducials for some certain metallicities have been obtained, while for other metallicities, the relationships between colors and absolute magnitudes has to be interpolated/extrapolated. Theoretical CMDs are calculated from stellar evolution models (e.g., Demarque et al. 2004; Girardi et al. 2004; Dotter et al. 2008). Therefore, we can get the color–magnitude relationship for any arbitrary metallicity (within the range of the stellar evolution models). Distances determined based on observational CMDs are sensitive to metallicities and colors, because only these two observables could be directly utilized. However, the accuracy of colors depends on the adopted reddening corrections, which are not easy to accurately determine. In this regard, it is more advantageous to use theoretical CMDs to determine distances, because effective temperature ($T_{\rm eff}$) and surface gravity ($\log g$) could be utilized to compensate for the effect of inaccurate colors. This is especially important to the data from the LAMOST survey because no homogenous photometry is available, and moreover, the LAMOST survey will cover a large amount of stars in the low Galactic latitude areas around the plane (Zhao et al. 2012) for which the reddening is significant. However, theoretical CMDs suffer from the disadvantage that they cannot fully reproduce the observations, especially for the giant stars (An et al. 2009).

This is the second in our series papers. Our first paper (Chen et al. 2014) presents a large and clean sample of red giant branch (RGB) stars selected from the ninth data release of SDSS (SDSS DR9, Ahn et al. 2012) based on the CH G band and MgH indices. The goal of this paper is to make a reasonable estimation of the distances to the sample stars, based on which the formation and evolution of the Galaxy could be studied. Moreover, we want to test whether the application of stellar parameters derived from low-resolution spectra could improve the determination of distances. If it works, the method could be applied to the data from the LAMOST survey. In the next section, we briefly describe the sample selection. Section 3 deals with the determinations of distances based on observational and theoretical CMDs (hereafter fiducials and isochrones), respectively, and a comparison between these two methods. Section 4 presents

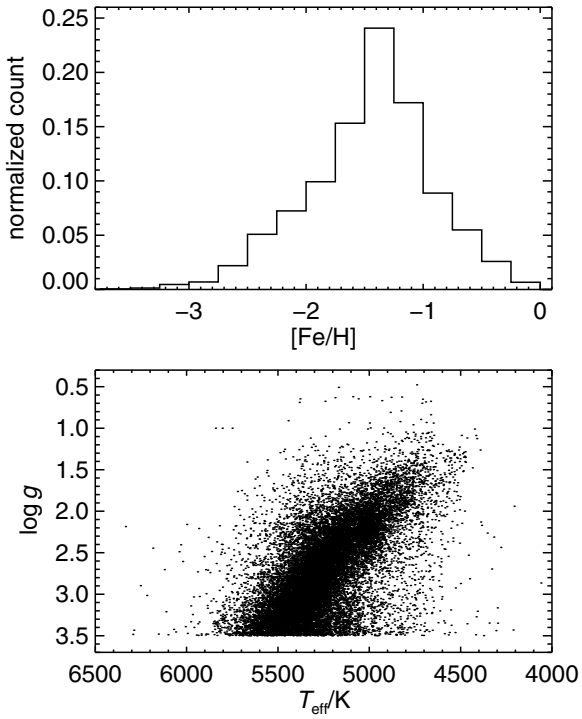

Figure 1. Upper panel: metallicity distribution of the sample stars. Lower panel: distribution of the sample stars in the Hertzsprung–Russell diagram.

the validation of our distance determinations with Galactic clusters. In Section 5, we compare our distances with those from previous investigations. A summary and conclusions are given in the last section.

2. THE SAMPLE

Our sample stars were selected from the SDSS DR9 database, which includes stars obtained during the original SDSS, the Sloan Extension for Galactic Understanding and Exploration (SEGUE; Yanny et al. 2009) in SDSS-II, and SEGUE-2 (Rockosi et al., in preparation) in SDSS-III. First, we limited our sample to stars whose spectra have signal-to-noise ratios (S/Ns) larger than 10. To eliminate early-type stars, we selected stars with effective temperatures between 3000 and 10,000 K. Then, stars with surface gravities less than 3.5 and $(g-r)_0$ between 0.4 and 1.0 were selected to ensure that most of the sample stars were RGB stars. At last, the same procedure described in Chen et al. (2013) was applied to remove the contamination of asymptotic giant branch stars or red horizontal branch stars in the relatively metal-poor region ([Fe/H] < -1.2) based on the CH(G) index; a similar procedure was applied in the relatively metal-rich region ([Fe/H] > -1.2) to remove the contamination of subgiant or dwarf stars based on the MgH index (Chen et al. 2014). We noted that some stars have multiple observations. For these stars, the spectra with the higher/highest S/Ns were adopted. Finally, we were left with 22,544 RGB stars. Figure 1 shows the distribution of stellar parameters for the sample stars.

Magnitudes and associated uncertainties in g and r bands given by the SDSS PHOTO pipeline were adopted, and $E(B-V)$ were estimated from Schlegel et al. (1998). Stellar parameters ($T_{\rm eff}$, log g, and [Fe/H]) and associated individual uncertainties needed for the distance computations were adopted from the updated and improved version of SEGUE Stellar Parameter Pipeline (SSPP; Lee et al. 2008a, 2008b; Allende Prieto et al. 2008; Smolinski et al. 2011; Lee et al. 2011a) catalog for SDSS DR9. One should keep in mind that the individual uncertainties for each stellar parameter delivered by SSPP are internal errors, which are estimated by averaging the parameters from multiple approaches. The median internal uncertainties of $T_{\rm eff}$, log g, and [Fe/H] for our sample stars are 49 K, 0.11 dex, and 0.04 dex, respectively. This is comparable to the typical internal errors claimed by Lee et al. (2008a), i.e., $\sigma(T_{\rm eff}) = 70$ K, $\sigma(\log g) = 0.18$ dex, and $\sigma([{\rm Fe/H}]) = 0.07$ dex, for stars in the range of 4500 K $\leqslant T_{\rm eff} \leqslant$ 7500 K. In addition to the internal errors, comparison with high-resolution spectroscopic analyses suggests that typical external errors for SSPP derived $T_{\rm eff}$, log g, and [Fe/H] are 141 K, 0.23 dex, and 0.23 dex, respectively (Lee et al. 2008a). Because it is unrealistic to assign a proper external uncertainty to each stellar parameter for each star, the computations of distances and associated uncertainties in the following are based only on the internal errors. Therefore, uncertainties of distances for individual stars given in the following should be lower than the real situations. However, we can estimate the typical uncertainty of distance for our sample stars based on the typical internal and external uncertainties of stellar parameters (see details in the next section).

Table 1
Metallicities, Reddening, and Distance Moduli of the Clusters

Cluster ID	[Fe/H]	$E(B-V)$	$(m-M)_0$
M92	-2.38^{a}	0.02^{a}	14.66^{b}
M13	-1.60^{a}	0.02^{a}	14.34^{b}
M71	-0.81^{a}	0.32^{a}	12.86^{b}
NGC 6791	$+0.40^{b}$	0.10^{b}	13.02^{b}

References. (a) Kraft & Ivans (2003); (b) An et al. (2009).

3. DETERMINATIONS OF DISTANCES

As mentioned above, both of the fiducials and isochrones have advantages and disadvantages in the distance determinations; thus, we decided to derive distances to the sample stars based on both of these methods, and then make a comparison.

3.1. Distances Based on Fiducials

We followed a very similar procedure to Xue et al. (2014) to derive distances using a Bayesian approach based on the fiducial sequences of Galactic globular and open clusters. Here, we only give a brief introduction to the procedure; for more details, please refer to Xue et al. (2014).

Fiducials of M92, M13, M71, and NGC 6791 in the $u'g'r'i'z'$ system from Clem et al. (2008) were adopted and were transformed to the $ugriz$ system using the transformation equations of Tucker et al. (2006). Table 1 gives the adopted metallicities, reddening, and distance moduli of the clusters. We did not use the fiducials in the native $ugriz$ system from An et al. (2008) because their fiducials are not as bright as those of Clem et al. (2008) in the RGB portion due to the saturation of stars brighter than $r \sim 14$ mag in the SDSS CCDs. It is obvious that the color–magnitude space is poorly sampled with fiducials for only four different metallicities; therefore, the relationships between color and magnitude for more [Fe/H] has to be interpolated or extrapolated. Following Xue et al. (2014), we adopted quadratic interpolations for metallicities within the boundaries, while, for [Fe/H] beyond the boundaries, since extrapolation is very uncertain, the lower or upper limits were simply adopted.

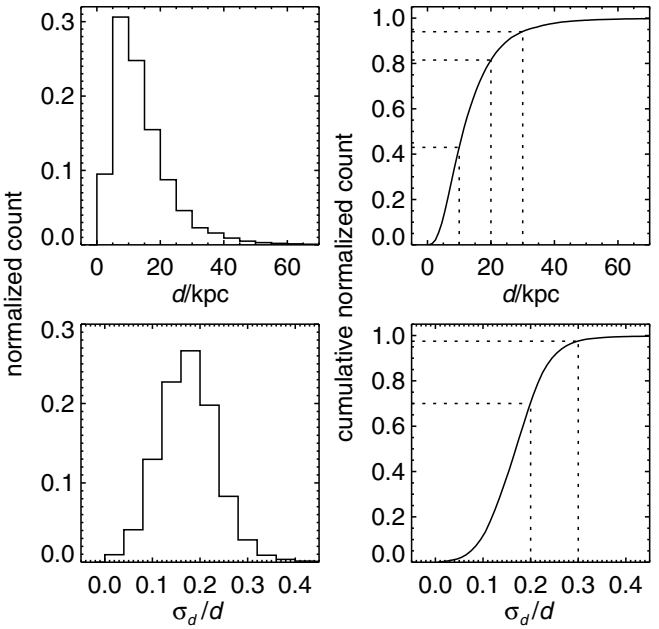

Figure 2. Distributions (left) and cumulative distributions (right) of the distances (upper) and associated relative uncertainties (lower) based on fiducials for the sample stars.

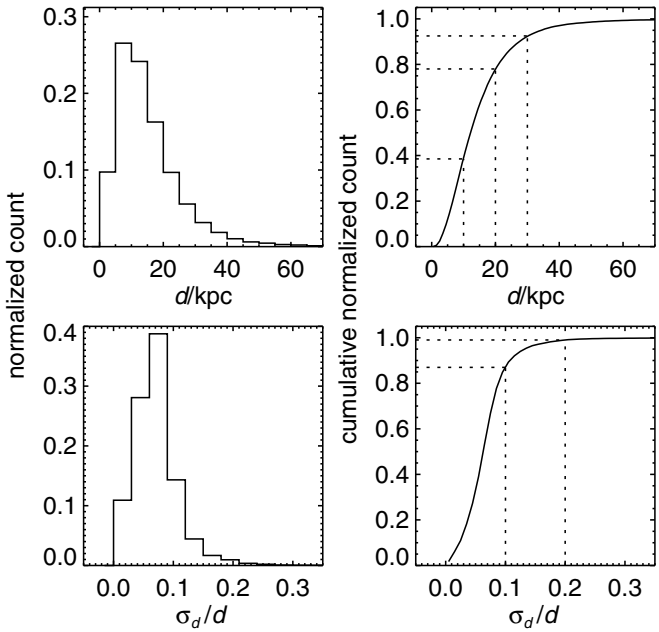

Figure 3. Same as Figure 2, but for the distances based on isochrones.

According to the Bayes' theorem, the posterior probability density function of the absolute magnitude (M) can be expressed as follows:

$$p(M|(g-r)_0, [\mathrm{Fe/H}]) \propto p((g-r)_0, [\mathrm{Fe/H}]|M)p(M), \quad (1)$$

where $p((g-r)_0, [\mathrm{Fe/H}]|M)$ is the likelihood and $p(M)$ the prior probability of M, or the luminosity function. The likelihood can be modeled with Gaussian functions as follows

$$p((g-r)_0, [\mathrm{Fe/H}]|M) \propto \exp\left(-\sum_i \frac{(q_i - q_i^{\mathrm{obs}})^2}{2\sigma_i^2}\right), \quad (2)$$

where q are the observables ($(g-r)_0$ or [Fe/H]) and σ the corresponding errors. For the luminosity function, we adopted the result $p(M) \propto 10^{0.32M}$ from Xue et al. (2014). The absolute magnitude could be connected with the observables ($(g-r)_0$ and [Fe/H]) by the fiducials described above. Then, we could get the probability density function (pdf) of the absolute magnitude. The pdf of the absolute magnitude are all Gaussian; thus, the peak and central 68% interval of the distribution were adopted as the most probable absolute magnitude and corresponding error, respectively. The distance and associated uncertainty could be further derived in combination with the apparent magnitude and associated uncertainty.

Some of the sample stars have colors beyond the range of the fiducials, and some have unreasonable (negative or zero) uncertainties for stellar parameters or colors. For these stars, we were not able to derive their distances. Finally, among the 22,544 sample stars, 22,337 have determined distances based on fiducials. Figure 2 shows the distributions and cumulative distributions of the distances as well as the associated relative uncertainties for these stars. It can be seen that the distribution of distances peaks at about 10 kpc with a tail extending to more than 70 kpc. About 80% of the sample stars have distances smaller than 20 kpc, and about 95% have distances smaller than 30 kpc. As we mentioned above, the uncertainties of distances shown in Figure 2 comes from the internal errors of stellar parameters only. If we add the typical internal and external errors in quadrature, then the typical relative uncertainty of distance for our sample stars would be 27%.

3.2. Distances Based on Isochrones

We adopted the same procedure as Carrell et al. (2012) to determine distances based on isochrones. This method was adapted from the procedure of Kordopatis et al. (2011), which is based on the method of Zwitter et al. (2010). We used the isochrones from Girardi et al. (2004). Because all of the stars in our sample are giants, we generated isochrones with a constant age of 10 Gyr. The grid of isochrones is linear from $Z = 0.0001$ ([Fe/H] $= -2.27$) to 0.03 ([Fe/H] $= 0.19$) in 0.0001 increments. To describe the extent of match between a point on the isochrone and a star with a given set of parameters, each point on the isochrone could be assigned with a Gaussian weight as follows:

$$w = \exp\left(-\sum_i \frac{(q_i - q_i^{\mathrm{obs}})^2}{2\sigma_i^2}\right), \quad (3)$$

where i corresponds to T_{eff}, $\log g$, [Fe/H], or $(g-r)_0$, q_i to the values from isochrones, q_i^{obs} to the values from observations, and σ_i to the measurement uncertainties. To correct the bias of untrue density distribution of stars along the isochrones, we associate an extra weight dm (mass step between two points of the same isochrones) to the previous one (refer to Kordopatis et al. 2011 and Zwitter et al. 2010 for more details). The absolute magnitude was then found from the weighted average of all points on the isochrones and the corresponding error was adopted from the weighted standard deviation. Then the distance and associated uncertainty were derived in combination with the apparent magnitude and associated uncertainty.

Due to the same reason described in the last paragraph of Section 3.1, we were not able to derive distances for some of the sample stars. At last, we get determined distances for 22,410 of the sample stars based on isochrones. Figure 3 shows the distributions and cumulative distributions of the isochrone-based distances as well as the associated relative uncertainties for

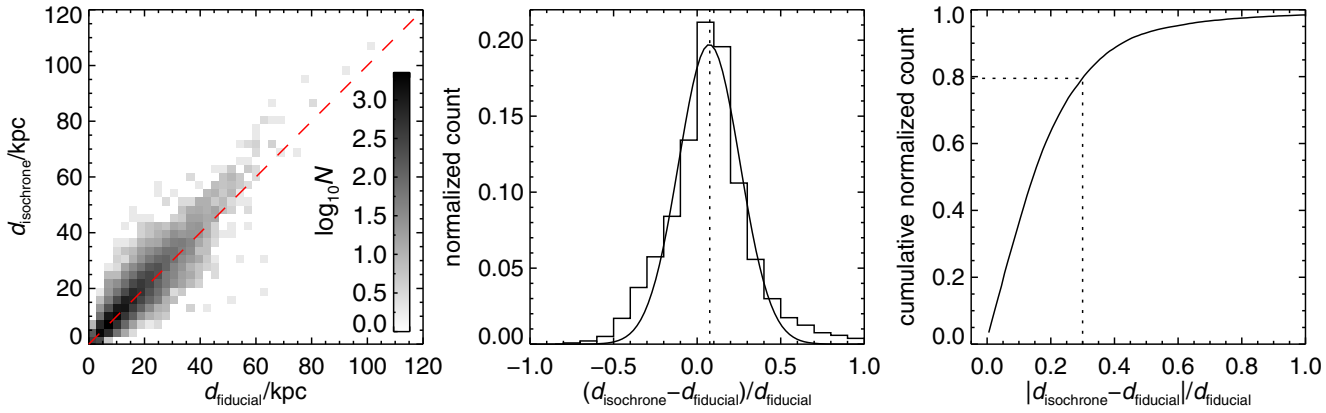

Figure 4. Left panel: density distribution of the sample stars in the isochrone- vs. fiducial-based distance plane. Middle panel: distribution of relative difference between isochrone- and fiducial-based distance for the sample stars. Right panel: cumulative distribution of absolute relative difference between isochrone- and fiducial-based distance for the sample stars.

(A color version of this figure is available in the online journal.)

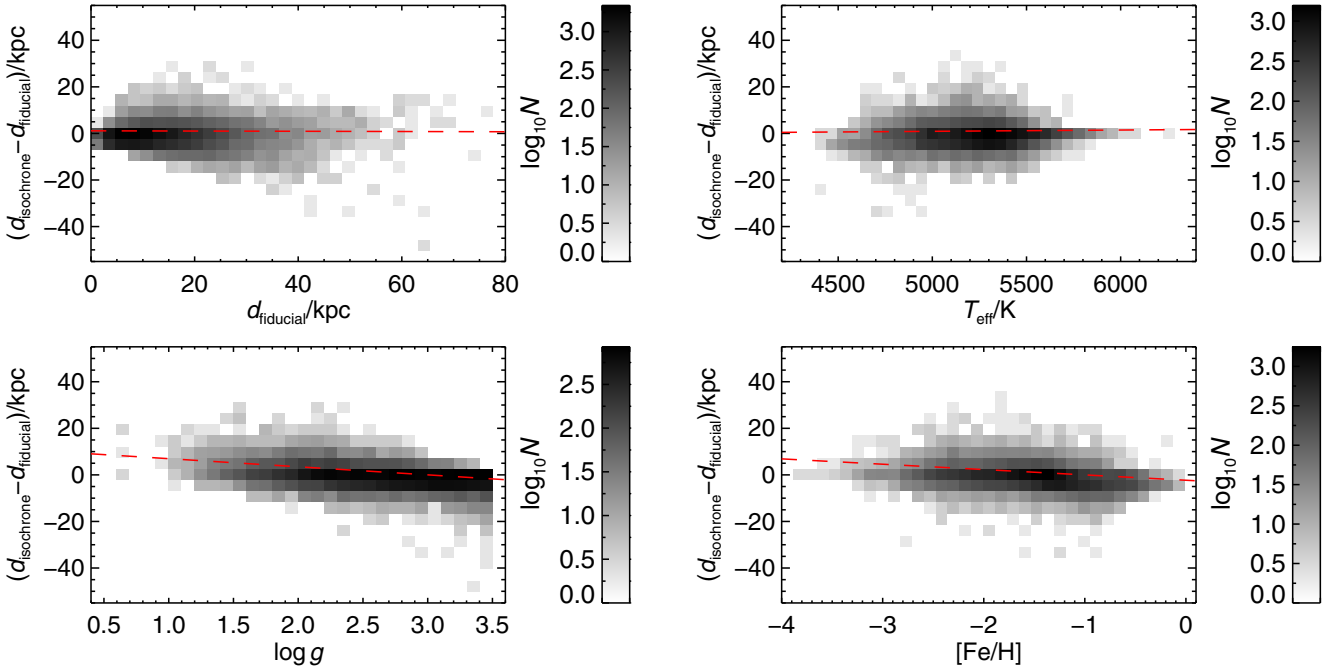

Figure 5. Density distribution of the sample stars in the distance offset (isochrone minus fiducial) vs. fiducial-based distance (upper left), effective temperature (upper right), surface gravity (lower left), and metallicity (lower right) plane. Dashed lines represent linear fits to the trends.

(A color version of this figure is available in the online journal.)

these stars. It can be seen that the distribution of distances is very similar to that based on fiducials (see more discussions on the comparison between the fiducial- and isochrone-based distances below). However, relative uncertainties of the distances based on isochrones are smaller than those based on fiducials. This should be due to the inclusion of more parameters ($T_{\rm eff}$ and log g) in distance calculations compared to the method based on fiducials. Still, the uncertainties of distances shown in Figure 3 comes from the internal errors of stellar parameters only. If we add the typical internal and external errors in quadrature, then the typical relative uncertainty of distance for our sample stars would be 19%.

3.3. Comparison between Fiducial- and Isochrone-based Distances

For 22,316 of the sample stars, we have determined distances from each of the two methods. Figure 4 shows the comparison between isochrone- and fiducial-based distances for these stars. The left panel demonstrates the general agreement between the distances from the two methods. The middle panel shows the distribution of relative differences between isochrone- and fiducial-based distances. We can see that distances based on isochrones are higher than those based on fiducials for the majority of the sample stars. The mean relative difference is 10% with a standard deviation of 31%, and the median relative difference is 8%. The right panel shows the cumulative distribution of absolute relative differences between distances from the two methods. It can be seen that for about 80% of the sample stars, the absolute relative differences are smaller than 30%.

Figure 5 shows the density distribution of the sample stars in the distance offset versus fiducial-based distance, effective temperature, surface gravity, and metallicity plane. We can see that there are no obvious relationships between distance offset and distance or between distance offset and effective

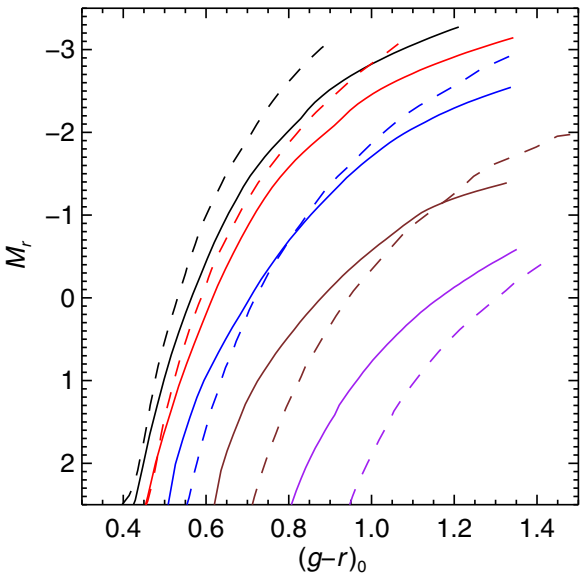

Figure 6. Comparison between interpolated cluster fiducials (solid) and theoretical isochrones (dashed) in RGB portions for [Fe/H] = −2.28 (black), −1.66 (red), −1.04 (blue), −0.42 (brown), and 0.20 (purple).

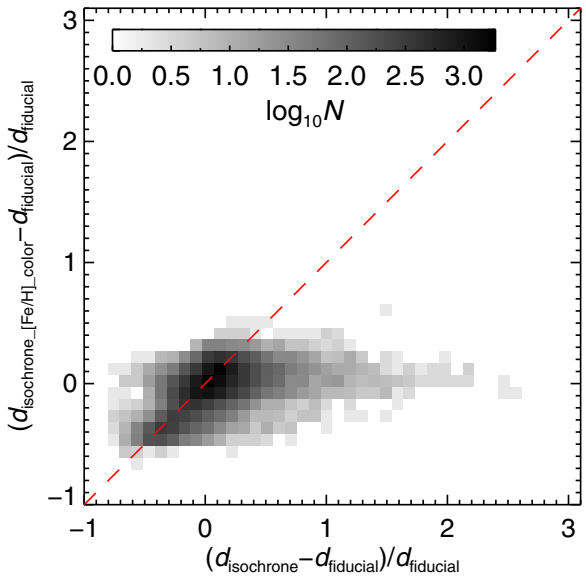

Figure 7. Density distribution of the sample stars in the relative difference between isochrone-based distance (only metallicities and colors are taken into account) and fiducial-based distance vs. relative difference between isochrone-based distance (all parameters taken into account) and fiducial-based distance plane.

temperature. However, a clear downward trend can be seen between distance offset and surface gravity; a similar trend also exists between distance offset and metallicity. This could be understood from Figure 6, which shows the comparison between interpolated cluster fiducials and theoretical isochrones in RGB portions for five different metallicities. It can be seen that, cluster fiducials and theoretical isochrones do not match well, and the difference varies with metallicity. More specifically, for a given color, theoretical isochrones are brighter than cluster fiducials at lower metallicities, while at higher metallicities, cluster fiducials are brighter than theoretical isochrones. Therefore, it is not surprising that distances based on fiducials are lower/higher than those based on isochrones in the metal-poor/metal-rich end as shown in the lower right panel of Figure 5. Because the offsets between fiducials and isochrones are not constant, it is impossible to make them match well for all metallicities with isochrones of a single age. However, the adoption of an age of 10 Gyr makes the difference in distance from the two methods minimum at [Fe/H] ~ -1, which is close to the peak of the distribution of [Fe/H] (-1.4) for the sample stars. It can also be seen in Figure 6 that, at lower metallicities (where most of the sample stars are located), offset between isochrone and fiducial increases with decreasing absolute magnitude. That is why we see a downward trend of distance offset with surface gravity in the lower left panel of Figure 5.

We noted that most of our sample stars should be halo/thick disk stars according to their metallicities. In this case, they should be enhanced in α-element abundance. This has a negligible effect on the distance determinations based on fiducials, because we used the "as-observed" fiducials (α-enhanced when [Fe/H] < 0 and solar-scaled when [Fe/H] > 0). However, the isochrones we used are based on solar-scaled compositions. Kim et al. (2002) shows that, at low metallicities, the effect of α enhancement can be approximated by increasing the metallicity. This means that distances to the sample stars with low metallicities will decrease if α enhancement is taken into account, and thus the offset between distances from fiducials and isochrones may be partially cancelled. Nevertheless, comparison with Galactic clusters shows that ignorance of α enhancement has only a very small influence on the accuracy of distance determinations based on isochrones (see details in Section 4).

Though distances from the two methods agree well for the majority of the sample stars, large offsets do exist for some of the stars. Differences between isochrones and fiducials should be partly responsible for this, but the most important reason is the introduction of effective temperature and surface gravity in the determination of distance based on isochrones. This can be proven in Figure 7. The abscissa of Figure 7 is the relative difference between isochrone-based distance (all parameters are taken into account) and fiducial-based distance, while the ordinate is the relative difference between isochrone-based distance (only [Fe/H] and color are taken into account) and fiducial-based distance. It can be seen that, when only [Fe/H] and color are taken into account in the determination of distance based on isochrones, the relative difference between the isochrone- and fiducial-based distance is restricted within 80%. However, when effective temperature and surface gravity are also introduced into the calculation of distance based on isochrones, the relative difference can be as high as 250%.

4. VALIDATION WITH GALACTIC CLUSTERS

In this section, we test the accuracy of our distance determinations with Galactic cluster member stars, which have well-determined distances. At first, we tried to make a comparison for the cluster member stars picked out from our sample stars (see our first paper for the selection criteria of cluster member stars). However, only 145 cluster member stars were picked out. We noted that a lot of cluster member stars presented in Smolinski et al. (2011) are not included in the SDSS data release. Among the 1,069 cluster member stars from Smolinski et al. (2011), 332 were identified as RGB stars by eye according to their positions on the CMDs. In order to make a more robust comparison with a larger sample, we decided to use the RGB cluster member stars from Smolinski et al. (2011) to test the accuracy of our distance determinations. We calculated distances

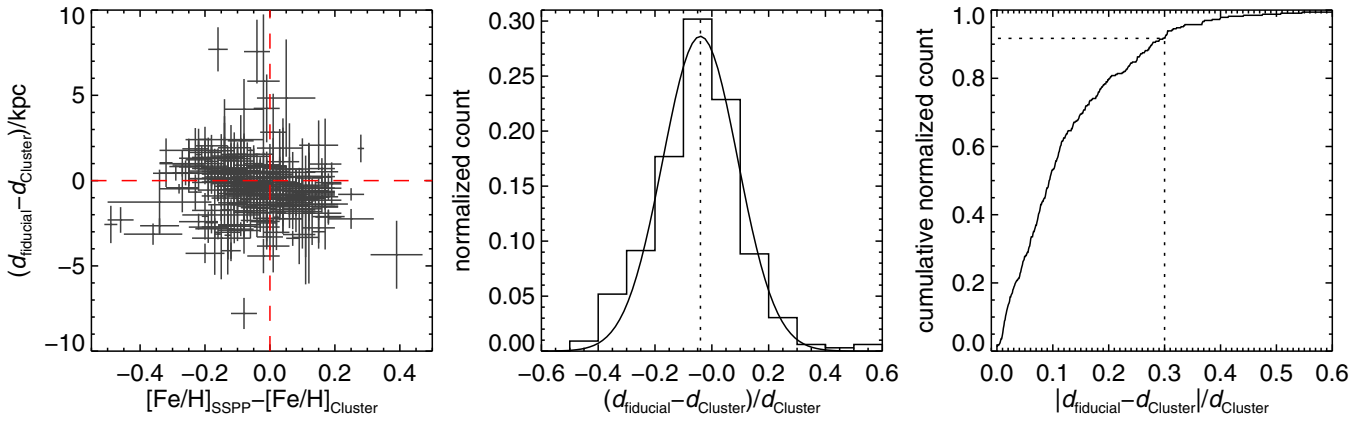

Figure 8. Left panel: difference between fiducial-based distance and literature distance as a function of difference between SSPP derived [Fe/H] and literature [Fe/H] for cluster member stars. Middle panel: distribution of relative difference between fiducial-based distance and literature distance for cluster member stars. Right panel: cumulative distribution of absolute relative difference between fiducial-based distance and literature distance for cluster member stars.

(A color version of this figure is available in the online journal.)

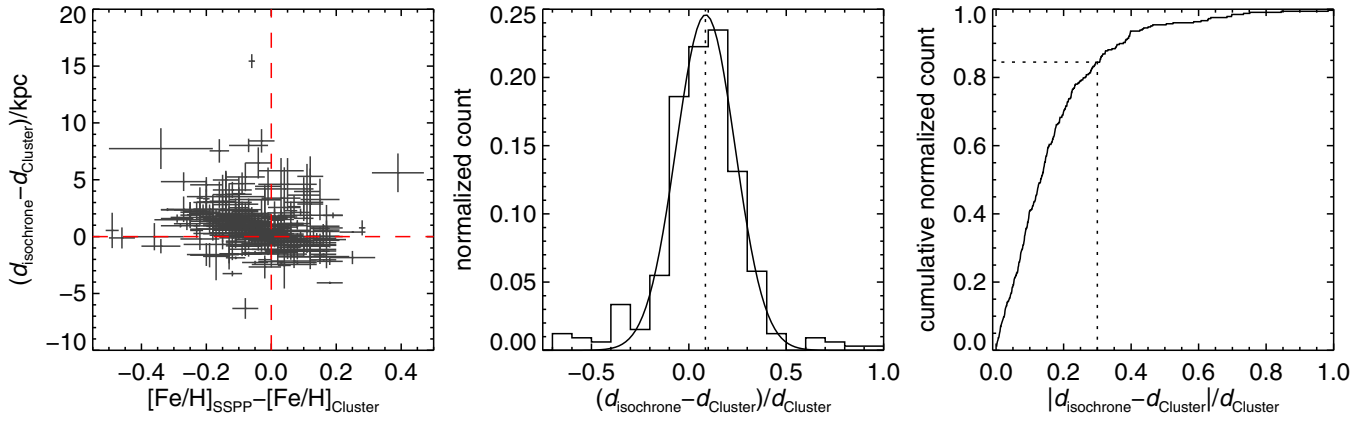

Figure 9. Same as Figure 8, but for the isochrone-based distances.

(A color version of this figure is available in the online journal.)

to these stars using the same methods as described in Section 3. Colors and stellar parameters needed for distance determination were adopted from Smolinski et al. (2011). Distances and metallicities were adopted from An et al. (2008) for globular (M2, M3, M13, M15, M53, M71, M92, and NGC 5053) and from Smolinski et al. (2011) for open clusters (NGC 2158 and NGC 6791).

Figure 8 shows the comparison between fiducial-based distance and literature distance for cluster member stars. The left panel shows the difference in distance versus offset in [Fe/H]; a clear downward trend can be seen as expected. The mean difference between the fiducial-based distance and literature distance is −0.4 kpc with a standard deviation of 1.6 kpc. The middle panel shows the distribution of relative difference between the fiducial-based distance and literature distance. It can be seen that, for the majority of the cluster member stars, fiducial-based distances are smaller than the literature distances. The mean relative difference is 4% with a standard deviation of 17%, and the median relative difference is 4%. The right panel shows the cumulative distribution of absolute relative difference between fiducial-based distance and literature distance for cluster member stars. It can be seen that for about 90% of the cluster member stars, the relative difference is smaller than 30%.

Figure 9 shows the comparison between isochrone-based distance and literature distance for cluster member stars. A downward trend between difference in distance and offset in [Fe/H] can also be seen in the left panel. The mean difference between the isochrone-based distance and literature distance is 0.9 kpc with a standard deviation of 2.0 kpc. As can be seen in the middle panel, for the majority of the cluster member stars, isochrone-based distances are larger than the literature distances. The mean relative difference is 8% with a standard deviation of 23%, and the median relative difference is 9%. For about 85% of the cluster member stars, the absolute relative difference is smaller than 30% as shown in the right panel.

As mentioned in the Introduction, one advantage of distance determination based on isochrones is that effective temperature and surface gravity could be taken into account to constrain the absolute magnitudes of stars. This is valid only if the derived effective temperature and surface gravity were accurate. The left panel of Figure 10 shows the absolute relative difference between fiducial-based distance and literature distance versus absolute relative difference between isochrone-based distance and literature distance for cluster member stars. For about 60% of the cluster member stars, distances based on fiducials are closer to the literature distances, while, for the rest of the stars, distances based on isochrones are closer to the literature distances. Therefore, the overall performance of distance determinations based on isochrones is not as good as that based on fiducials. This could be due to the intrinsic differences between isochrones and fiducials, or due to the inaccurate effective temperature or surface gravity introduced into the calculation of

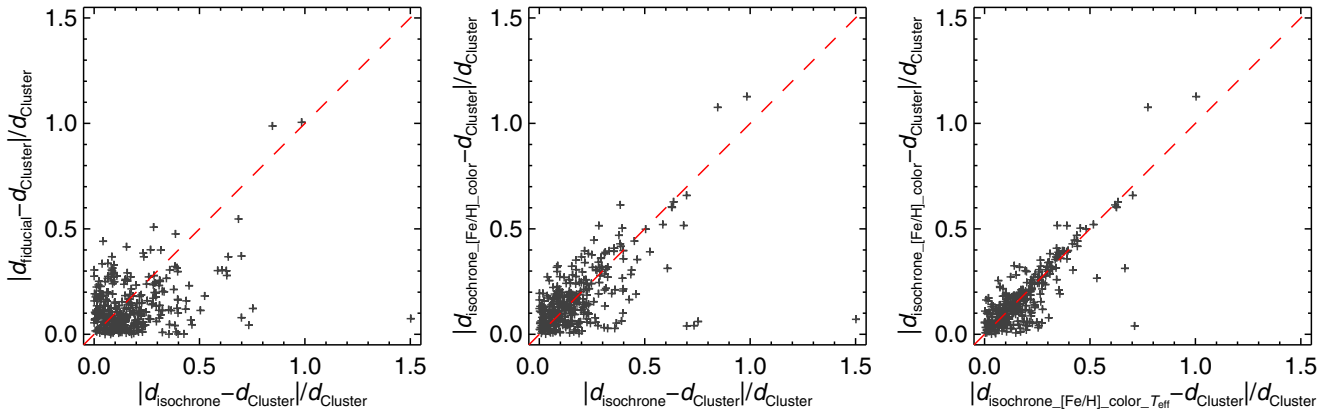

Figure 10. Left panel: absolute relative difference between fiducial-based distance and literature distance vs. absolute relative difference between isochrone-based distance and literature distance for cluster member stars. Middle panel: absolute relative difference between isochrone-based distance (only [Fe/H] and $(g-r)_0$ taken into account) and literature distance vs. absolute relative difference between isochrone-based distance (all parameters taken into account) and literature distance for cluster member stars. Right panel: absolute relative difference between isochrone-based distance (only [Fe/H] and $(g-r)_0$ taken into account) and literature distance vs. absolute relative difference between isochrone-based distance ([Fe/H], $(g-r)_0$, and $T_{\rm eff}$ taken into account) and literature distance for cluster member stars.

(A color version of this figure is available in the online journal.)

distance based on isochrones, or both. To investigate the effect of effective temperature and surface gravity on distance determinations based on isochrones, we also calculated distances to cluster member stars based on isochrones without the consideration of $T_{\rm eff}$ and $\log g$ (i.e., only [Fe/H] and $(g-r)_0$ are taken into account), and compare them with the distances also based on isochrones, but with all parameters included. The results are shown in the middle panel of Figure 10. We found that, when effective temperature and surface gravity are taken into account, deviations of calculated distances from the literature values become smaller for only 54% of the cluster member stars. This suggests that the inclusion of effective temperature and surface gravity does not improve the accuracy of distance determinations very much, which could be due to the fact that the $T_{\rm eff}$ and $\log g$ are not accurate enough. As an example, we can see from the middle panel of Figure 10 that for some stars, distances based on isochrones with only [Fe/H] and $(g-r)_0$ included deviate from the literature distances by no more than 10%, but when $T_{\rm eff}$ and $\log g$ are also included, the deviations can be as high as 150%. To examine the effect of effective temperature and surface gravity on distance determinations separately, we also calculate distances based on isochrones taking into account [Fe/H], $(g-r)_0$, and $T_{\rm eff}$, but not $\log g$. The results are compared with the distances based also on isochrones, but with only [Fe/H] and $(g-r)_0$ included in the right panel of Figure 10. We can see that the scatter between the two distance scales is obviously smaller than that in the middle panel of Figure 10, and several stars with peculiarly large distance deviations appearing in the middle panel disappear in the right panel. This indicates that, compared to effective temperature, surface gravity given by the SSPP is more likely to be inaccurate. This is not unexpected because it is relatively easier to derive accurate effective temperature than surface gravity from low-resolution spectra.

As an example, Figure 11 shows two member stars from M2 whose distances, based on isochrones with all parameters included, deviate from the literature distance by 70%. Such differences are far beyond the uncertainties introduced by the errors of input parameters (less than 20%). However, distances for these two stars, also based on isochrones but taking into account only [Fe/H] and $(g-r)_0$, agree with the literature distance very well, with relative differences of less than 5%. Effective temperatures of these two stars need to increase by 270 and 130 K, respectively, and surface gravities need to increase by 0.33 and 0.65 dex, respectively, to reproduce the literature distance.

As we mentioned in the Introduction, distance determination using only metallicity and color suffers from the problem of inaccurate reddening for stars with significant interstellar extinction. In this regard, effective temperature and surface gravity derived from spectroscopy may help to better constraint the distance. As a test, we compare different distance scales for member stars from four clusters (M15, M71, NGC 2158, and NGC 6791) with high reddening ($E(B-V) \geqslant 0.1$). The results are shown in Figure 12. We can see from the left panel of Figure 12 that, when both $T_{\rm eff}$ and $\log g$ are taken into account, the performance of distance determination does not improve. For half of the stars, distances with all parameters included get closer to the literature values, while the opposite is the case for the other half. However, as shown in the right panel of Figure 12, when $\log g$ is excluded, the ratio of stars with distances closer to the literature values than those with only [Fe/H] and $(g-r)_0$ included increases to 64%. This suggests that for stars with high reddening, inclusion of effective temperature could improve the accuracy of derived distance to some extent.

5. COMPARISON WITH OTHER INVESTIGATIONS

We note that there are already computed distances for the SDSS/SEGUE stars in the SSPP catalog, which are based on the calibrations of Beers et al. (2000). The strategy of their calibrations is to sort the stars into different luminosity classes according to their surface gravities first, and then derive their absolute magnitudes from a set of fiducials of Galactic clusters. Because all of our sample stars have $\log g < 3.5$, we extracted the distances for giants from the SSPP catalog, and compared them with those determined in this work. The upper panel of Figure 13 shows the distribution of relative difference in distance between SSPP and this work for the sample stars. It can be seen that for the majority of the sample stars, distances given by SSPP are smaller than those determined in this work. The median relative difference is 24% and 28% for the distances based on fiducials and isochrones, respectively. To further investigate which distance scale is closer to the reality, we compared the distances given by SSPP and this work with the literature distances for the 145 Galactic cluster member stars in

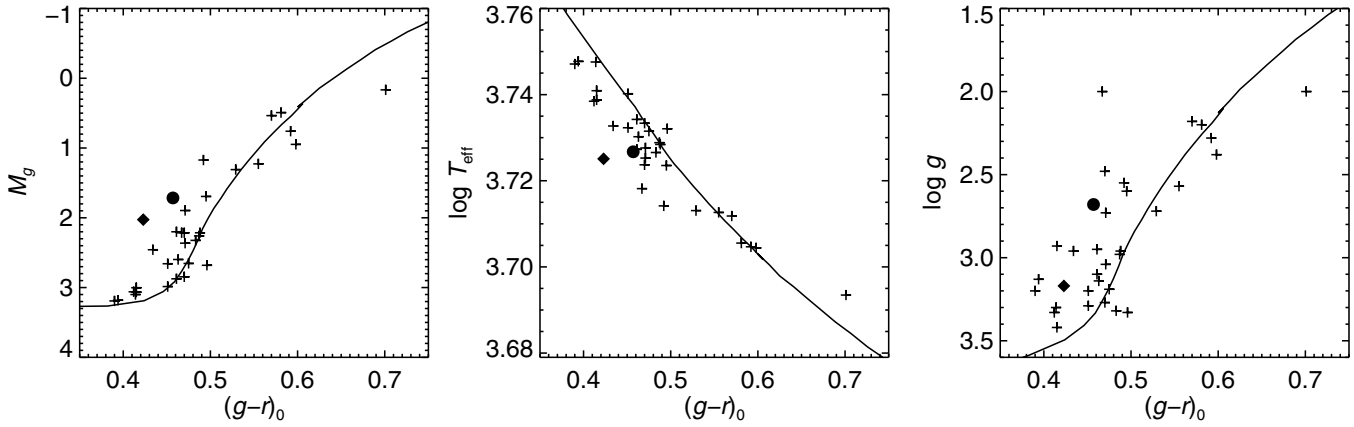

Figure 11. Comparison between observational quantity and theoretical isochrone for member stars from M2. The solid line represents theoretical isochrone with [Fe/H] = −1.68. Diamonds and circles represent the two stars ([Fe/H] = −1.69 and −1.65, respectively) whose distances are based on isochrones (all parameters taken into account) having the largest deviation from the literature distance. Other stars from M2 are marked with pluses for reference.

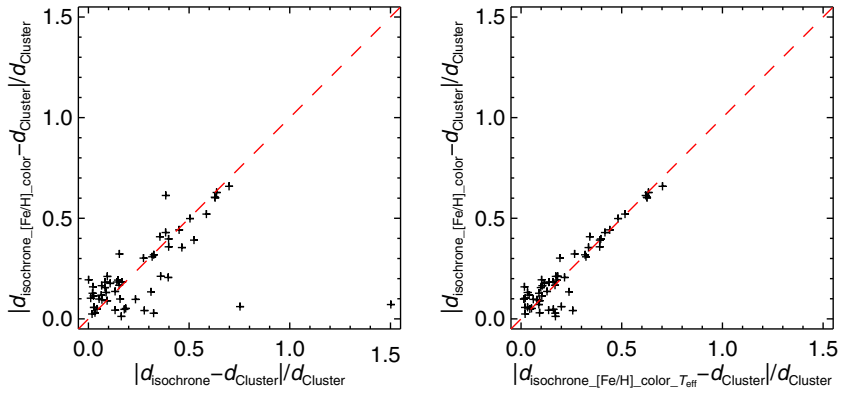

Figure 12. Left panel: absolute relative difference between isochrone-based distance (only [Fe/H] and $(g-r)_0$ taken into account) and literature distance vs. absolute relative difference between isochrone-based distance (all parameters taken into account) and literature distance for cluster member stars with high reddening. Right panel: absolute relative difference between isochrone-based distance (only [Fe/H] and $(g-r)_0$ taken into account) and literature distance vs. absolute relative difference between isochrone-based distance ([Fe/H], $(g-r)_0$, and $T_{\rm eff}$ taken into account) and literature distance for cluster member stars with high reddening.
(A color version of this figure is available in the online journal.)

the sample. The results are shown in the lower panel of Figure 13. We can see that distances based on fiducials and isochrones from this work show better agreement with the literature distances than those given by SSPP in terms of the spread as well as the peak of the distribution of relative deviations. We noted that our distances based on fiducials show larger deviations from the literature cluster distances than our isochrone-based distances. It is possible that the literature cluster distances were mainly based on isochrones.

Recently, Xue et al. (2014) presented an online catalog of distances for 6036 K giants from SDSS/SEGUE, of which 4557 are included in our sample. We compared the distances from Xue et al. (2014) with those based on fiducials from this work for the common stars. The result shows that distances from the two works are in excellent agreement; the mean relative difference is 3% with a standard deviation of 2%. This is not surprising since we used very similar procedure and fiducials. Distances from Xue et al. (2014) are slightly smaller than those from this work, which should be due to the fact that they used an extra prior (metallicity distribution function) that is not included in this work.

As an external test, we also calculated distances to the giant stars extracted from the fourth data release of RAVE (Kordopatis et al. 2013a), and compared them with those adopted by RAVE. Distances reported in RAVE were based on an improved Bayesian method taking into account the interstellar extinction and kinematic correction factors (see Binney et al. 2014a for details). Because RAVE targets stars with 2MASS photometry, we need fiducials or isochrones in the 2MASS JHK_s system. Unfortunately, there were no sufficient cluster fiducials in the JHK_s system with different metallicities to interpolate. Therefore, we could only calculate distances to RAVE stars based on isochrones. We generated isochrones similar to that described in Section 3.2, but in the JHK_s system. Stellar parameters, colors, extinctions, as well as associated errors were extracted from the RAVE DR4 catalog. The upper panel of Figure 14 shows the relative differences in distances between those determined with our procedure and those by Binney et al. (2014a) for 235,600 giant stars from RAVE. It can be seen that for the majority of the stars, distances from the two methods are in reasonable agreement, though our distances are about 10% lower than those from Binney et al. (2014a). The middle panel of Figure 14 shows the density distribution of the RAVE giant stars in the relative difference in distance versus distance plane. It can be seen that the relative difference shows a decreasing trend with increasing distance, and, in particular, distances from Binney et al. (2014a) are obviously higher than those determined with our procedure for lots of stars closer than 2 kpc. Because RAVE covers a lot of bright stars, some of them may have accurate parallaxes that

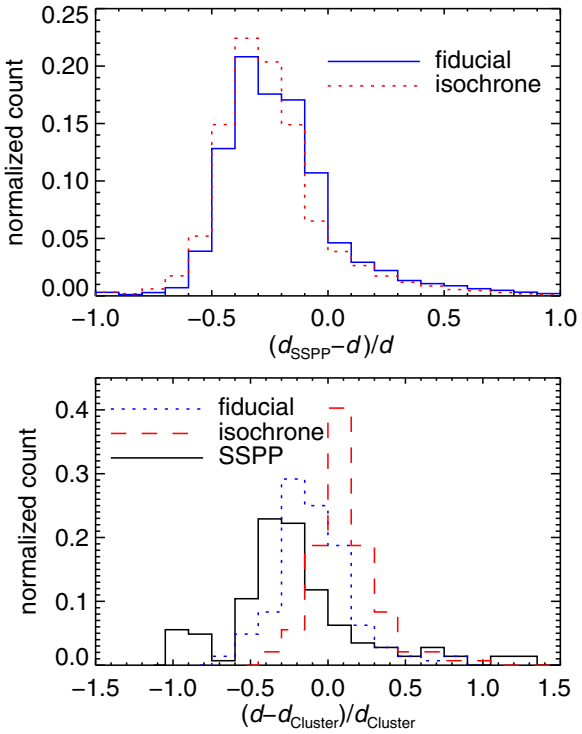

Figure 13. Upper panel: distribution of relative differences in distances between SSPP and this work for the sample stars. Lower panel: distribution of relative deviations from the literature distances for 145 Galactic cluster member stars in the sample.

(A color version of this figure is available in the online journal.)

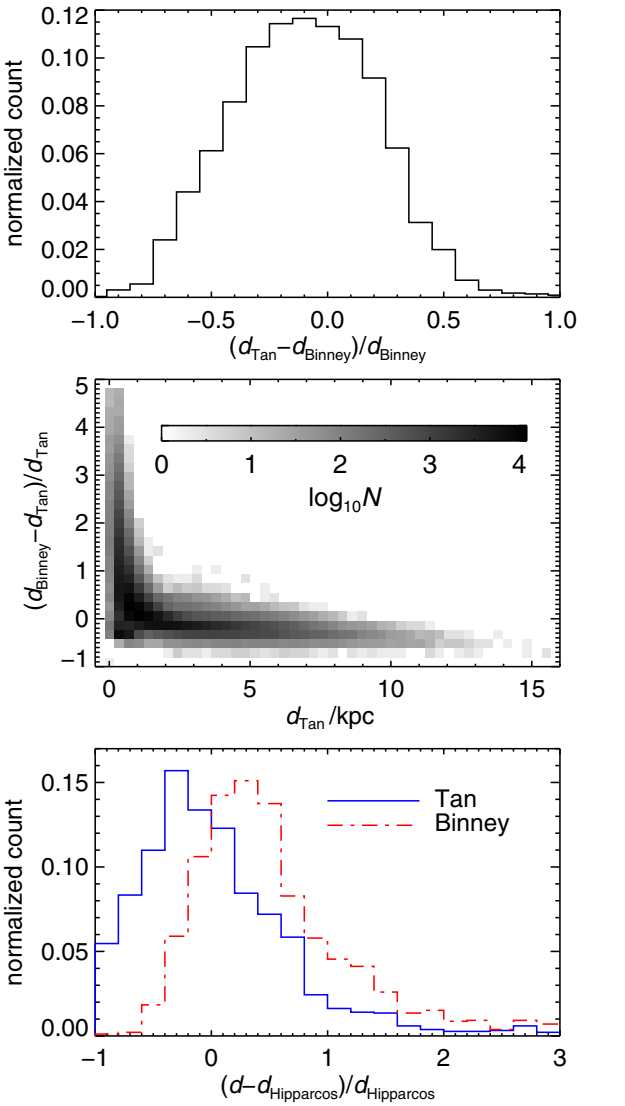

Figure 14. Upper panel: distribution of relative differences in distances between those determined with our procedure and those by Binney et al. (2014a) for the giant stars from RAVE. Middle panel: density distribution of the RAVE giant stars in the relative difference in distance vs. distance plane. Lower panel: distribution of relative deviations from the *Hipparcos* distances for the RAVE giant stars with *Hipparcos* parallaxes.

(A color version of this figure is available in the online journal.)

could be used to test the validity of distance determinations. We cross-matched the giant stars with the *Hipparcos* catalog (van Leeuwen 2007) using a search radius of one arcsec. After removing stars with relative errors in parallax lager than 50%, we are left with 1847 stars. The lower panel of Figure 14 shows the distribution of relative deviations from the distances based on *Hipparcos* parallaxes for these stars. It can be seen that our procedure tends to underestimate the distances, while Binney et al. (2014a) tends to overestimate distances to the giant stars. The result is the same if the comparison is restricted to the stars of which the relative uncertainties in parallaxes are lower than 20%. Binney et al. (2014a) also noted their overestimation of distances to giant stars, which may be due to the priors they adopted. The underestimation of our distance determinations should be due to the isochrones we adopted. As can be seen in Figure 6, observational cluster fiducials are brighter than theoretical isochrones at metal-rich ends, and most of the RAVE stars are relatively metal-rich (distribution of [Fe/H] peaks at about −0.3). That is why our distances are underestimated. Therefore, the isochrones we adopted are not suitable for determining distances to stars with relatively high metallicities. However, as we have discussed in Section 3.3, this does not affect the SDSS sample investigated in this work very much because most of them are metal-poor stars.

6. SUMMARY

In this work, we have determined distances for a large and clean sample of RGB stars selected from the SDSS DR9 based on both observational cluster fiducials and theoretical isochrones. Distribution of distances based on fiducials peaks at about 10 kpc with a tail extending to more than 70 kpc. The typical relative uncertainty of distances based on fiducials is about 27%. Distribution of distances based on isochrones is very similar to that based on fiducials, but the corresponding errors are smaller than those based on fiducials due to the inclusion of two extra parameters ($T_{\rm eff}$ and $\log g$). The typical relative uncertainty of distances based on isochrones is about 19%. A comparison of distances from the two methods shows that for about 80% of the sample stars, the absolute relative differences between distances from the two methods are smaller than 30%; though, for the majority of the sample stars, distances based on isochrones are larger than those based on fiducials with a median relative difference of 8%. Differences in distances from the two methods show a clear trend with $\log g$ and [Fe/H], which is mainly due to the differences between fiducials and isochrones. We find that the relative difference in distance from the two methods can be as high as 250% for some of the sample stars, which is caused by the inclusion of $T_{\rm eff}$ and $\log g$ in the distance

Table 2
Parameters of the Sample Stars

Plate	MJD	Fiber	α (deg)	δ (deg)	[Fe/H]	$\sigma_{\rm [Fe/H]}$	$T_{\rm eff}$ (K)	$\sigma_{T_{\rm eff}}$ (K)	log g	$\sigma_{\log g}$	RV (km s^{-1})
268	51633	46	149.6984	−0.6662	−1.23	0.00	5360	49	3.19	0.11	170.1
268	51633	57	149.9805	−0.4972	−1.42	0.04	5433	44	3.23	0.09	175.2
270	51909	145	152.7498	−0.3804	−2.77	0.05	5520	31	1.76	0.85	64.1
272	51941	75	156.8150	−0.2579	−2.44	0.04	5402	47	2.34	0.11	284.3
272	51941	211	155.6261	−0.8317	−1.25	0.06	5411	38	2.88	0.01	230.0

g_0 (mag)	$(g-r)_0$ (mag)	σ_g (mag)	σ_r (mag)	$d_{\rm fid}$ (kpc)	$\sigma_{d_{\rm fid}}$ (kpc)	$d_{\rm iso}$ (kpc)	$\sigma_{d_{\rm iso}}$ (kpc)	$d_{\rm iso\_[Fe/H]\_color\_}T_{\rm eff}$ (kpc)	$\sigma_{d_{\rm iso\_[Fe/H]\_color\_}T_{\rm eff}}$ (kpc)	$d_{\rm iso\_[Fe/H]\_color}$ (kpc)	$\sigma_{d_{\rm iso\_[Fe/H]\_color}}$ (kpc)
17.672	0.537	0.017	0.018	12.00	2.36	9.57	0.74	9.34	0.99	10.62	1.97
17.512	0.477	0.021	0.019	7.38	1.66	8.48	0.54	8.19	0.59	8.65	1.35
18.619	0.454	0.017	0.019	16.38	3.97	15.81	0.88	15.71	0.85	20.00	4.18
17.276	0.471	0.014	0.012	11.55	2.11	15.67	1.16	11.54	1.35	12.51	2.29
17.850	0.496	0.016	0.012	9.11	1.69	14.94	0.32	8.71	0.73	9.11	1.26

Notes. The first three columns give the plate number, Modified Julian Date, and fiber ID. Right ascension and declination are given in the next two columns. Stellar atmospheric parameters (metallicity, effective temperature, and surface gravity) and errors are given in the next six columns. Heliocentric radial velocity is given in the next column. Magnitude in g band, $(g-r)$ color, and errors in g and r band magnitudes are given in the next four columns (subscript 0 means extinction corrected). The last eight columns give the distance based on fiducials, distance based on isochrones with all parameters included, distance based on isochrones with [Fe/H], $(g-r)_0$ and $T_{\rm eff}$ included, distance based on isochrones with only [Fe/H] and $(g-r)_0$ included, and associated uncertainties.

(This table is available in its entirety in a machine-readable form in the online journal. A portion is shown here for guidance regarding its form and content.)

determinations based on isochrones. If we ignore these two parameters, the relative difference will be restricted within 80%.

We test the accuracy of our distance determinations with Galactic globular and open cluster member stars. The results show that for about 90% of the cluster member stars, the absolute relative difference between our fiducial-based distances and the literature values is smaller than 30%, and the corresponding ratio is 85% for the isochrone-based distances. We investigate the effect of effective temperature and surface gravity on distance determinations and find that the inclusion of these two parameters does not improve the accuracy of distances very much. Our results show that effective temperature and, especially, surface gravity derived from low-resolution spectra are not accurate enough to improve the accuracy of distance determinations. However, for stars with significant interstellar extinction, the inclusion of effective temperature may help to improve the accuracy of derived distances to some extent.

Distances to our sample stars are available from an online catalog. For the sake of reliability, not all the sample stars are presented in the catalog. Only those stars with relative errors in distance less than 30%, and with deviations between distances from the two methods (fiducials versus isochrones with [Fe/H], $(g-r)_0$, and $T_{\rm eff}$ included) less than 30%, enter the catalog. The final catalog consists of 17,941 stars. Table 2 shows the first five rows of the catalog for guidance. Figure 15 shows the spatial distribution of the sample stars in the catalog. The large size of sample with reasonable distance estimations, in combination with large distance coverage makes our sample suitable for the investigation of the formation and evolution of the Galaxy, especially the Galactic halo.

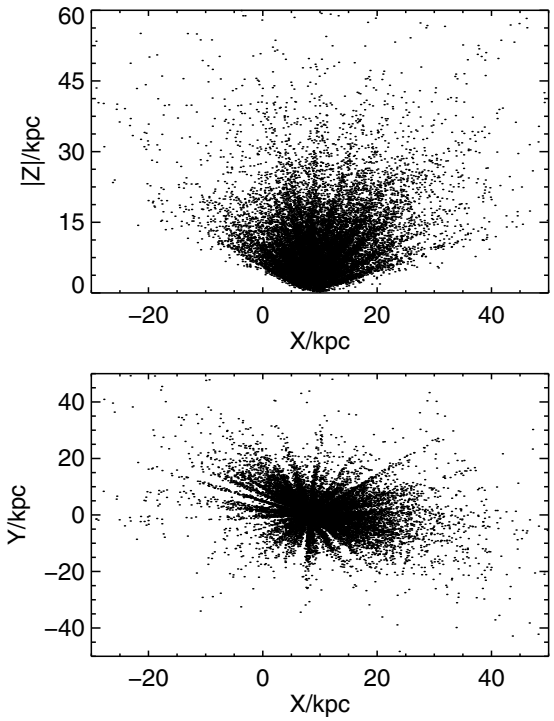

Figure 15. Spatial distribution of the sample stars in the catalog.

We are grateful to the anonymous referee for valuable suggestions and comments. This work is supported by the National Nature Science Foundation of China under grant Nos. 11103034, 11222326, 11233004, 11390371, U1331120, and U1431106, and by the National Basic Research Program of China under grant No. 2014CB845701/03. This research has made use of the cross-match service provided by CDS, Strasbourg and NASA's Astrophysics Data System.

Funding for SDSS-III has been provided by the Alfred P. Sloan Foundation, the Participating Institutions, the National Science Foundation, and the U.S. Department of Energy Office of Science. The SDSS-III Web site is http://www.sdss3.org/.

SDSS-III is managed by the Astrophysical Research Consortium for the Participating Institutions of the SDSS-III Collaboration, including the University of Arizona, the Brazilian Participation Group, the Brookhaven National Laboratory, Carnegie Mellon University, the University of Florida, the French Participation Group, the German Participation Group, Harvard University, the Instituto de Astrofisica de Canarias, the Michigan

State/Notre Dame/JINA Participation Group, Johns Hopkins University, Lawrence Berkeley National Laboratory, the Max Planck Institute for Astrophysics, the Max Planck Institute for Extraterrestrial Physics, New Mexico State University, New York University, Ohio State University, Pennsylvania State University, the University of Portsmouth, Princeton University, the Spanish Participation Group, the University of Tokyo, the University of Utah, Vanderbilt University, the University of Virginia, the University of Washington, and Yale University.

Facility: Sloan

REFERENCES

Ahn, C. P., Alexandroff, R., Allende Prieto, C., et al. 2012, ApJS, 203, 21
Allende Prieto, C., Sivarani, T., Beers, T. C., et al. 2008, AJ, 136, 2070
An, D., Johnson, J. A., Clem, J. L., et al. 2008, ApJS, 179, 326
An, D., Pinsonneault, M. H., Masseron, T., et al. 2009, ApJ, 700, 523
Beers, T. C., Chiba, M., Yoshii, Y., et al. 2000, AJ, 119, 2866
Binney, J., Burnett, B., Kordopatis, G., et al. 2014a, MNRAS, 437, 351
Binney, J., Burnett, B., Kordopatis, G., et al. 2014b, MNRAS, 439, 1231
Brown, T. M., Ferguson, H. C., Smith, E., et al. 2005, AJ, 130, 1693
Carollo, D., Beers, T. C., Chiba, M., et al. 2010, ApJ, 712, 692
Carrell, K., Chen, Y., & Zhao, G. 2012, AJ, 144, 185
Chen, Y. Q., Zhao, G., Carrell, K., et al. 2014, ApJ, in press
Chen, Y. Q., Zhao, G., Carrell, K., Zhao, J. K., & Tan, K. F. 2013, ApJ, 765, 156
Clem, J. L., VandenBerg, D. A., & Stetson, P. B. 2008, ApJ, 135, 682
Cui, X.-Q., Zhao, Y.-H., Chu, Y.-Q., et al. 2012, RAA, 12, 1197
Demarque, P., Woo, J.-H., Kim, Y.-C., & Yi, S. K. 2004, ApJS, 155, 667
Dotter, A., Chaboyer, B., Jevremović, D., et al. 2008, ApJS, 178, 89
Girardi, L., Grebel, E. K., Odenkirchen, M., & Chiosi, C. 2004, A&A, 422, 205
Ivezić, Ž., Sesar, B., Jurić, M., et al. 2008, ApJ, 684, 287
Jurić, M., Ivezić, Ž., Brooks, A., et al. 2008, ApJ, 673, 864
Kim, Y.-C., Demarque, P., Yi, S. K., & Alexander, D. R. 2002, ApJS, 143, 499
Kordopatis, G., Gilmore, G., Steinmetz, M., et al. 2013a, AJ, 146, 134
Kordopatis, G., Gilmore, G., Wyse, R. F. G., et al. 2013b, MNRAS, 436, 3231
Kordopatis, G., Recio-Blanco, A., de Laverny, P., et al. 2011, A&A, 535, A107
Kraft, R. P., & Ivans, I. I. 2003, PASP, 115, 143
Lee, Y. S., Beers, T. C., Allende Prieto, C., et al. 2011a, AJ, 141, 90
Lee, Y. S., Beers, T. C., An, D., et al. 2011b, ApJ, 738, 187
Lee, Y. S., Beers, T. C., Sivarani, T., et al. 2008a, AJ, 136, 2022
Lee, Y. S., Beers, T. C., Sivarani, T., et al. 2008b, AJ, 136, 2050
Perryman, M. A. C., Lindegren, L., Kovalevsky, J., et al. 1997, A&A, 323, L49
Schlegel, D. J., Finkbeiner, D. P., & Davis, M. 1998, ApJ, 500, 525
Smolinski, J. P., Lee, Y. S., Beers, T. C., et al. 2011, AJ, 141, 89
Steinmetz, M., Zwitter, T., Siebert, A., et al. 2006, AJ, 132, 1645
Tucker, D. L., Kent, S., Richmond, M. W., et al. 2006, AN, 327, 821
van Leeuwen, F. 2007, A&A, 474, 653
Wilson, M. L., Helmi, A., Morrison, H. L., et al. 2011, MNRAS, 413, 2235
Xue, X.-X., Ma, Z., Rix, H.-W., et al. 2014, ApJ, 784, 170
Yanny, B., Rockosi, C., Newberg, H. J., et al. 2009, AJ, 137, 4377
York, D. G., Adelman, J., Anderson, J. E., Jr., et al. 2000, AJ, 120, 1579
Zhao, G., Zhao, Y.-H., Chu, Y.-Q., Jing, Y.-P., & Deng, L.-C. 2012, RAA, 12, 723
Zwitter, T., Matijevič, G., Breddels, M. A., et al. 2010, A&A, 522, A54